

氧化釧，氧化鐳及氧化鉛高介電層特性之研究

研究生：林盈彰


指導教授：黃調元 博士

簡昭欣 博士

國立交通大學

電子工程學系 電子研究所碩士班

摘要



根據半導體的微縮定律，隨著元件持續的微小化，極薄的二氧化矽介電層將伴隨著極大的直接穿遂漏電流，而此直接穿遂漏電流將對元件的功率消耗有嚴重的影響。在閘極二氧化矽介電層薄至 1 奈米以下時，為解決此一嚴重的直接穿遂漏電流現象，勢必須利用高介電係數材料來替換傳統的二氧化矽。因為高介電係數材料在相同的等效二氧化矽厚度時，具有較大的實際物理厚度，故可降低直接穿遂漏電流。

近幾年，有很多研究在探討二氧化鉛介電層的特性。但最近稀土金屬氧化物如氧化釧和氧化鐳也開始受到重視。由於目前相關文獻不多，故在論文中，我們試著用物理沈積的方法，去製作氧化釧和氧化鐳介電層，並對其做一些基本電性的研究。

相較於前二者，二氧化鉛介電層已被研究很久。因此在論文中，

我們對二氧化鉛介電層施以低溫氨氣的氮化處理($\sim 400\text{ }^{\circ}\text{C}$), 來提昇其電特性。並對有低溫氨氣處理的試片做一些電性分析, 如漏電流、崩潰電場和電性逼迫處造成之漏電流等等。最後從我們的實驗結果顯示, 低溫氨氣處理在提昇二氧化鉛的特性上確是一個可行的方法。



The study of Electrical Properties on La_2O_3 , Pr_2O_3 and HfO_2 Gate Dielectrics

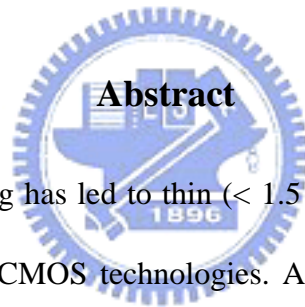
Student : Ying-Chang Ling

Advisor : Dr. Tiao-Yuan Huang

Dr. Chao-Hsin Chien

Department of Electronics Engineering and Institute of Electronics

National Chiao Tung University, Hsinchu, Taiwan



Abstract

Aggressive device scaling has led to thin (< 1.5 nm) silicon dioxide (SiO_2) gate dielectrics in state-of-the-art CMOS technologies. As a result, static leakage power due to direct tunneling through the gate oxide has been increasing at an exponential rate. As technology roadmaps call for sub-15Å gate oxides within the next five years, a variety of alternative high- k materials are being investigated as possible replacements for SiO_2 . The higher dielectric constant in these materials allows the use of physically thicker films, thus potentially reducing the tunneling current while maintaining the gate capacitance needed for scaled device operation.

In the last few years, much work has been done to understand the properties of HfO_2 gate dielectrics. More recently, rare earth metal oxides such as amorphous La_2O_3 and epitaxial Pr_2O_3 films deposited on Si substrates have received much attention. In

this thesis, we used physical vapor deposition (PVD) method to deposit La_2O_3 and Pr_2O_3 gate dielectrics and studied the electrical characteristics of these gate dielectrics.

HfO_2 films as potential gate dielectric have been studied for a long time. In this thesis, low temperature (~ 400) NH_3 treatment on HfO_2 gate dielectrics was used to improve the electrical properties. Electrical characteristics of HfO_2 gate dielectrics including leakage current, breakdown field, and stress induced leakage current (SILC) were measured on samples with low temperature nitridation. Our results show that the low temperature treatment appears to be an effective method to improve the HfO_2 gate dielectrics.



誌 謝

論文可以順利完成，要感謝很多人的協助，其中特別要向黃調元教授、簡昭欣博士、林鴻志博士致上最高的敬意與感謝，從他們身上學習到做人做事該有的謹慎、細膩、積極與負責等不可缺之精神。當然也讓我在專業知識上有更深的啟發。

此外，要感謝實驗室所有的師兄弟，李耀仁學長、葉冠麟學長、呂嘉裕學長、李明賢學長、俊榮、景森在研究的過程中互相切磋指教，特別感謝盧文泰學長、林育賢學長在實驗設計、量測跟論文討論上提供熱心的指教與建議，還有柏青、慶宗、久盟、楊明瑞學長、沈士文學長、黃英傑學長，藍文廷學弟、李聰杰學弟在實驗過程中的鼎力相助。

在兩年的過程中經歷了喜悅、歡樂、挫折與灰心，直到最後可以順利完成，要再次感謝以上的夥伴與師長們的陪伴與支持。

最後要感謝父母與家中所有成員，在這一路上不斷地鼓勵與協助，讓我不斷成長與進步。

Contents

Abstract (Chinese)	I
Abstract (English)	III
Acknowledgements	V
Contents	VI
Table Captions	VIII
Figure Captions	IX

Chapter 1 Introduction

1.1 Background.....	1
1.2 The Choice of High-k Materials.....	3
1.3 Motivation.....	7
1.4 Thesis Organization.....	8

Chapter 2 Characterizations of E-Beam-Deposition La_2O_3 , Pr_2O_3

High-k Thin Films on Si substrates

2.1 Introduction	10
2.2 Experiment(I)	11
2.3 Results and Discussion(I).....	12
2.3.1 Electrical properties of La_2O_3 gate dielectrics	12
2.3.2 Frequency dispersion	13
2.3.3 Current density as a function of temperature	14
2.3.4 TEM.....	15

2.4 Experiment (II)	16
2.5 Results and Discussion (II).....	16
2.5.1 Electrical properties of Pr ₂ O ₃ gate dielectrics	16
2.6 Summary.....	18
Chapter 3 Effects of Low-Temperature NH₃ Treatment on HfO₂/SiO₂	
Stack Gate Dielectrics by MOCVD	
3.1 Introduction.....	20
3.2 Experimental procedure.....	21
3.3 Results and Discussion.....	23
3.3.1 Electrical properties of HfO ₂ gate dielectrics.....	23
3.3.1.1 C-V & I-V characteristics.....	23
3.3.2 Transmission electron microscopy (TEM).....	27
3.3.3 Frequency dispersion.....	28
3.3.4 Reliability characteristics.....	29
3.3.5 Summary.....	32
Chapter 4 Conclusions and Suggestions for Future Work	
4.1 Conclusions.....	34
4.2 Future Work	36
References	37

Table Captions

Table. 1-1 Criteria and requirements for high-k dielectric materials to be used as gate dielectric. [4]

Table. 3-1 Split conditions



Figure Captions

Chapter 1

Fig 1-1. Bandgaps of some well-known high-k materials

Chapter 2

Fig.2-1. Cross-sectional view and key experimental procedures of the test structure.

Fig.2-2. C-V characteristics of La_2O_3 films fabricated with different PDA for control samples.

Fig.2-3. C-V characteristics of La_2O_3 films fabricated with different PDA for RTO-treated samples.

Fig.2-4. EOT for various RTA temperatures

Fig.2-5. Leakage current density for various RTA temperatures.

Fig.2-6 (a) C-V curves measured at multiple frequencies for control samples without RTA.

(b) C-V curves measured at multiple frequencies for control samples with 600 °C RTA.

(c) C-V curves measured at multiple frequencies for control samples with 700 °C RTA.

(d) C-V curves measured at multiple frequencies for control samples with 800 °C RTA.

Fig.2-7(a) C-V curves measured at multiple frequencies for RTO samples without RTA .

(b) C-V curves measured at multiple frequencies for RTO samples with 600°C RTA.

(c) C-V curves measured at multiple frequencies for RTO samples with 700°C RTA.

(d) C-V curves measured at multiple frequencies for RTO samples with 800°C RTA.

Fig.2-8 (a). J-V characteristics as a function of temperature.

(b) Leakage current at -0.5V plotted as a function of inverse temperature, the solid line is a fit to the experimental data.

Fig.2-9 (a) TEM image of control sample without RTA treatment.

(b) TEM image of control sample with 600°C RTA.

(c) TEM image of RTO sample with 600°C RTA.

Fig.2-10 (a). C-V characteristics of Pr_2O_3 films with various RTA PDA and no sintering.

(b) Gate current density vs. gate voltage. The plot shows J-V characteristics of Pr_2O_3 gate dielectrics.

Fig.2-11 EOT variation of samples with sintering and no-sintering according to annealing temperature N2 for 60s.

Fig.2-12. Leakage current density variation of samples with sintering and no-sintering according to annealing temperature N2 for 60s.

Fig.2-13. Hysteresis as a function of RTA temperature for samples with (square) and without (circle) sintering.

Fig.2-14 (a). TEM image of sample without RTA treatment.

(b) TEM image of sample with RTA treatment at 600°C

Chapter 3

Fig. 3-1. Cross-sectional view and key experimental procedures of the test structure.

Fig. 3-2. Gate capacitance vs. gate voltage. The plot shows high frequency C-V curves of the control samples with various RTA temperatures

Fig. 3-3. Gate capacitance vs. gate voltage. The plot shows high frequency C-V curves of the TN samples with various RTA temperatures

Fig. 3-4. Gate capacitance vs. gate voltage. The plot shows high frequency C-V curves of the BN samples with various RTA temperatures

Fig. 3-5: J-V characteristics of the control samples with various RTA temperatures.

Fig. 3-6: J-V characteristics of the BN samples with various RTA temperatures.

Fig. 3-7: J-V characteristics of the TN samples with various RTA temperatures.

Fig. 3-8: The comparison of leakage current density among the control, BN and TN samples at RTA 700 .

Fig. 3-9: The leakage current distribution of different treatment at 700 .

Fig.3-10 (a) TEM image of control samples without RTA treatment.

(b) TEM image of control samples with RTA at 600 °C .

(c) TEM image of control samples with RTA at 700 °C .

(d) TEM image of TN samples with RTA at 700 °C .

Fig.3-11(a) C-V curves measured at multiple frequencies of control samples without RTA.

(b) C-V curves measured at multiple frequencies of control samples with RTA at 600 .

(c) C-V curves measured at multiple frequencies of control samples with RTA at 700 °C.

Fig.3-12(a) C-V curves measured at multiple frequencies of TN samples without RTA.

(b) C-V curves measured at multiple frequencies of TN samples with RTA at 600 °C.

(c) C-V curves measured at multiple frequencies of TN samples with RTA at 700 °C.

Fig.3-13: The Weibull plots of breakdown field for the control samples with various RTA treatments.

Fig.3-14: The Weibull plots of breakdown field for the TN samples with various RTA treatments.

Fig.3-15(a) SILC result of control sample under constant field (15.8MV/cm) stressing for as-deposited.

(b) SILC result of control sample under constant field (15.8MV/cm) stressing for 600 °C RTA.

(c) SILC result of control samples under constant field (15.8MV/cm) stressing for 700 °C RTA.

Fig.3-16(a) SILC result of TN samples under constant field (15.8MV/cm) stressing for as-deposited.

(b) SILC result of TN samples under constant field (15.8MV/cm) stressing for 600 °C RTA.

(c) SILC result of TN samples under constant field (15.8MV/cm) stressing for 700 °C RTA.

Fig.3-17 Trap generation rate $((J-J_0)/J_0)\%$ (J at $V_g=-1V$) against stress time for

control and TN samples with various RTA treatments.

Fig.3-18 (a) The C-V curves before and after constant voltage stress in HfO_2 gate dielectrics for control sample without RTA treatment

(b) The C-V curves before and after constant voltage stress in HfO_2 gate dielectrics for control sample with $600^\circ C$ RTA.

(c) The C-V curves before and after constant voltage stress in HfO_2 gate dielectrics for control sample with $700^\circ C$ RTA.

Fig.3-19(a) The C-V curves before and after constant voltage stress in HfO_2 gate dielectrics for TN sample without RTA .

(b) The C-V curves before and after constant voltage stress in HfO_2 gate dielectrics for TN sample with $600^\circ C$ RTA.

(c) The C-V curves before and after constant voltage stress in HfO_2 gate dielectrics for TN sample with $700^\circ C$ RTA.

Fig.3-20 (a) J-V curves as a function of temperature for control samples without RTA treatment.

(b) J-V curves as a function of temperature for control samples with $600^\circ C$ RTA.

(c) J-V curves as a function of temperature for control samples with $700^\circ C$ RTA.

Fig.3-21 (a) J-V curves as a function of temperature for TN samples without RTA.

(b) J-V curves as a function of temperature for TN samples with $600^\circ C$ RTA.

(c) J-V curves as a function of temperature for TN samples with $700^\circ C$ RTA.